International Journal of Engineering Innovation & Research
Volume 10, Issue 4, ISSN: 2277 – 5668

Study on Active Collision Avoidance System Based on Estimation of Peak Road Adhesion Coefficient

Peilin Shi, Longhui Zhou*, Jianwei Hou, Minglei Liang, Liaodong Zheng and Yushuai Zhao
School of Transportation and Vehicle Engineering Shandong University of Technology, Shandong, Zibo, Zhangdian, 255049, China.
*Corresponding author email id: 759767868@qq.com

Date of publication (dd/mm/yyyy): 17/07/2021

Abstract **– In order to improve the driving safety of vehicles, this paper designed an active vehicle collision avoidance system based on the estimation method of road peak adhesion coefficient and the combination of longitudinal braking collision avoidance and lane changing to avoid collision. In the case that the vehicle running straight on the low adhesion road is about to rear-end collision with the vehicle in front, and the driver fails to respond in time, the system can independently decide the way of collision avoidance by identifying the adhesion condition of the road, control the vehicle steering or braking, avoid the rear-end collision, and expand the application scope of the vehicle collision avoidance system.**

Keywords **– Low Adhesion Road Surface, Peak Road Adhesion Coefficient, Longitudinal Braking to Avoid Collision, Turn to Another Lane to Avoid A Collision.**

I. INTRODUCTION

With the development of the automobile industry, traffic safety has become the focus of more and more attention, and the active safety of the automobile has also become the focus of research by the majority of researchers. At present, there are two active safety methods to avoid rear-end collision in straight line driving: longitudinal braking to avoid collision and lane changing to avoid collision. Longitudinal braking has a relatively low impact on the surrounding traffic environment, and is the mainstream solution to avoid collisions in the market at present. However, the decrease of braking efficiency caused by low adhesion road surface seriously restricts its performance of collision avoidance. The way of lane changing is more advantageous in low adhesion road surface and high relative speed of front and rear vehicles to avoid collision. It can avoid collision in a relatively short distance, but the condition of road surface adhesion restricts the safety and stability of lane changing process. If the estimation of the low adhesion road surface is not accurate enough, it may lead to more serious accidents if the steering method is adopted rashly to avoid collision. In view of this, this paper proposes using the road adhesion coefficient estimation method is effective to estimate the road adhesion conditions and using the identification result set up to evaluate the low adhesion road longitudinal braking under the condition of collision avoidance and steering in collision avoidance of security model, implement active collision avoidance system reasonable mode of collision avoidance, to give full play to the advantages of two types of collision avoidance.

II. ESTIMATION OF PEAK ADHESION COEFFICIENT OF ROAD SURFACE

According to different test means and measurement parameters, estimation algorithms of road adhesion coefficient can be roughly divided into cause-based estimation algorithm and effect-based estimation algorithm [1]. The cause-based estimation algorithm measures the roughness of the road surface and identifies the road surface by adding pavement recognition sensors. The accurate sensor combined with the specific recognition algorithm can accurately estimate the road adhesion coefficient. This kind of method has high identification

accuracy, which can be estimated in real time and obtain accurate parameters without vehicle acceleration or braking operation. However, it needs to add road identification sensors, which requires high hardware requirements.

The effect-based estimation algorithm estimates the current road surface adhesion coefficient by measuring the vehicle state response caused by the change of the adhesion conditions between the road surface and the tire. The estimation algorithm based on the braking force coefficient-slip rate curve can estimate the actual braking force coefficient without the installation of complex road identification sensors. Although the estimation value obtained by this method is prone to large errors when the wheel slip rate is low, the estimation result of this method is accurate when the wheel slip rate is high and can meet the requirements.

Due to the low road adhesion coefficient, the braking performance of the vehicle is insufficient. When the vehicle is braking, ABS can keep the slip rate of the wheel near the slip rate corresponding to the peak road adhesion coefficient. At this point, the peak adhesion coefficient of road surface is representative of the road surface adhesion conditions to some extent. Therefore, the method to estimate the peak adhesion coefficient of road surface based on the braking force coefficient-slip ratio curve can be used to estimate the peak adhesion coefficient of low-adhesion road surface by the active collision avoidance system.

Burckhardt model was adopted in this paper. Based on a large number of vehicle road test data, this model was summarized to represent the functional relationship between the longitudinal braking force coefficient and the longitudinal tire slip rate [2], as shown in Equation 1.

$$\varphi(s) = C_1(1-\exp(-C_2 s)) - C_3 s \tag{1}$$

Where, φ is the braking force coefficient; S is wheel slip rate; C_1, C_2 and C_3 are the corresponding parameter values of the adhesion coefficient curves of each typical road surface, and the specific parameters are shown in Table 1.

Table1 Typical pavement characteristic parameter values.

The Road Surface Type	C_1	C_2	C_3
Dry asphalt	1.281	23.93	0.520
Dry cement	1.196	25.17	0.537
Wet asphalt	0.856	33.82	0.347
Wet cobblestones	0.400	33.71	0.120
snow	0.195	94.13	0.065
Ice	0.050	306.39	0.001

By substituting the parameters in Table 1 into Formula 1, the function curve of braking force coefficient-slip rate of six typical road surfaces can be obtained, as shown in Fig. 1.

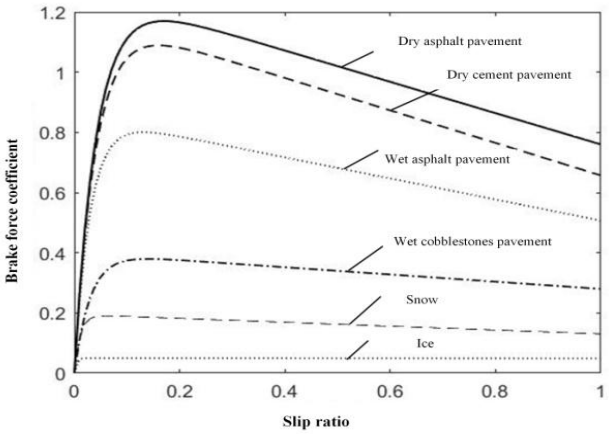

Fig. 1. Braking force coefficient - slip rate curve.

As can be seen from Fig. 1, when wheel slip rate is very low, curves of typical road surface are very close to each other, making it difficult to identify. When the wheel slip rate is within the range of [0.1, 1], the curves of different typical road surfaces can be clearly distinguished. This paper realizes the estimation of the peak adhesion coefficient of road surfaces through this characteristic.

In order to verify the accuracy of the model, the Burckhardt model adopted in this paper needs to be compared and verified with the curve of braking force coefficient-slip rate of typical road surface in the Carsim software. The curve of braking force coefficient-slip rate of typical road surface in the Carsim software is shown in Fig. 1.

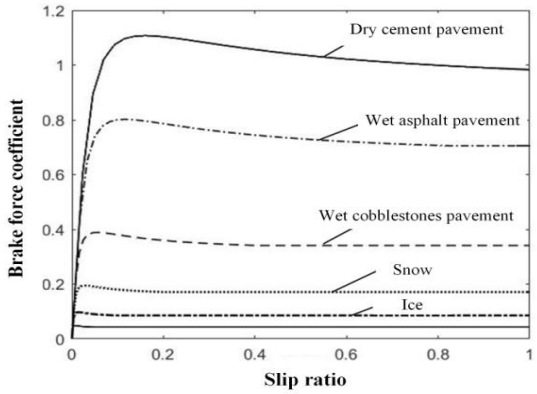

Fig. 2. Braking force coefficient - slip rate curve.

As shown in Fig. 2, because it is very difficult to obtain the wheel braking force coefficient in the range of high slip rate on the road surface with high peak adhesion coefficient of road surface, this paper only obtained the typical road utilization adhesion coefficient curve between dry cement road surface and ice road surface in CarSim. By comparing the utilization adhesion coefficient curves of dry cement, wet asphalt, wet cobblestone and other pavement in Figure 2 and Figure 1, the curve variation trend in the range of 0 to 0.4 slip rate is basically similar to that of Burckhardt model. Therefore, it is considered that Burckhardt model can accurately describe the relationship between tire slip rate and road utilization adhesion coefficient.Since the slip rate and braking force coefficient are constantly changing in the braking process, the two parameters need to be processed to estimate the peak adhesion coefficient of the road surface, so the estimation method as shown in Fig. 3 is adopted.

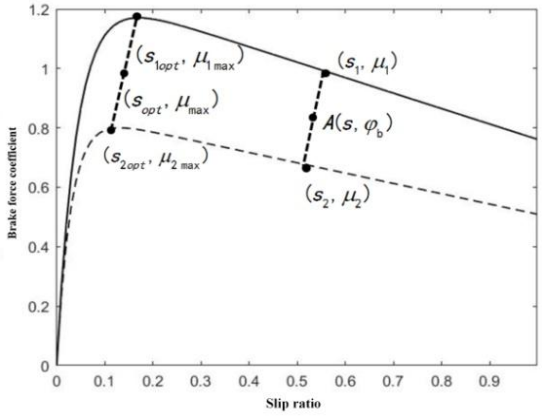

Fig. 3. Braking force coefficient - slip rate curve.

As shown in Figure 3, the collected data points can be divided into two types: one is that they fall on the typical road surface curve, in which case the peak adhesion coefficient of the road surface can be determined by an accurate function curve; One is that it falls between the curves of typical road surface. At this time, the peak adhesion coefficient of road surface needs to be determined by the estimation algorithm set. Assuming the collected data point A fall between six tire-road friction curve, due to lack of data points in A road - brake force coefficient of slip ratio function curve, unable to accurately get the current peak road adhesion coefficient of road surface, but according to the figure 1 presents the regularity of the curve, can be concluded that data point A corresponding braking force coefficient - slip rate function curve between two adjacent typical curve, and the value of the peak adhesion coefficient of the road surface is also between the value of the peak adhesion coefficient of the adjacent typical road surface. According to the above laws, the peak adhesion coefficient of the identified target road surface can be estimated through Equations 2 and 3.

$$\varphi_{max} = \frac{\varphi_b - \varphi_2}{\varphi_1 - \varphi_2} \cdot \varphi_{1max} + \frac{\varphi_b - \varphi_1}{\varphi_2 - \varphi_1} \cdot \varphi_{2max} \tag{2}$$

$$\frac{\varphi_b - \varphi_1}{s - s_1} = \frac{\varphi_b - \varphi_2}{s - s_2} = \frac{\varphi_{2max} - \varphi_{1max}}{s_{2opt} - s_{1opt}} \tag{3}$$

Where, φ_{max}, φ_{1max} and φ_{2max} are the peak adhesion coefficients of the current road surface and two typical road surfaces adjacent to it. S_{1opt} and S_{2opt} are the slip rates corresponding to the peak adhesion coefficient of two typical adjacent road surfaces. φ_b is the braking force coefficient to be identified at present; S_1, S_2, φ_1 and φ_2 are the slip rates and braking force coefficients on the adhesion curves of two adjacent road surfaces.

To realize the above calculation method, the wheel slip rate and road surface adhesion coefficient need to be calculated. In the braking process, the slip rate is calculated as shown in Equation 4.

$$s = \frac{v_w - \omega_w \cdot R_e}{v_w} \tag{4}$$

Where, S is wheel slip rate; ω_w is the wheel angular velocity; v_w is the wheel center speed; R_e is the wheel rolling radius.

In the process of vehicle braking, the braking force coefficient of the wheel is calculated as shown in Equation 5:

$$\varphi_b = \frac{F_x}{F_z} \tag{5}$$

Where, F_x is the longitudinal force on the wheel; F_z is the vertical load of the wheel.

The longitudinal force calculation of the wheel requires the force analysis of a single wheel, as shown in Fig. 4.

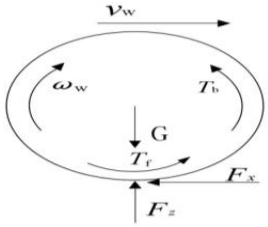

Fig. 4. Force analysis of single wheel.

According to the tire force analysis in Figure 4, the longitudinal force exerted by the road surface on the wheel can be expressed in Formula 6:

$$F_x = \frac{J_w \dot{\omega}_w + T_b + T_f}{r} \tag{6}$$

Where, Jw is the rotational inertia of the wheel; TB is the braking torque; Tf is the rolling resistance moment.

$$F_{zfl} = \frac{mgb}{2(a+b)} - \frac{ma_x h}{2(a+b)} - \frac{ma_y hb}{(a+b)B_w} \tag{7}$$

In the formula, B_w is the vehicle wheel base; h is the height of vehicle center of mass; a_x is the longitudinal acceleration of the vehicle; a_y is the lateral acceleration of vehicle; a is the distance from the center of mass to the front axis; b is the distance from the center of mass to the rear axis; F_{zfl} is the vertical load of the left front wheel; g is the acceleration of gravity.

Due to the identification algorithm of road surface peak adhesion coefficient adopted in this chapter, a large amount of computation will be generated in the identification process, which is not conducive to real-time estimation. In order to improve the calculation efficiency, the peak adhesion coefficient corresponding to different slip rates and braking force coefficient is calculated, and then the peak adhesion coefficient of the current road surface is estimated by lookup table method.

Due to the limited sample data of the typical pavement adhesion curve, the braking force coefficient that is too small or too large may be unable to estimate the peak adhesion coefficient because there is no typical sample data as a reference. Therefore, when the braking force coefficient is larger than the curve of dry asphalt pavement or smaller than the curve of ice pavement, the estimation algorithm is simplified, as shown in Equation 8:

$$\varphi_{max}(s,\varphi) = \begin{cases} \varphi_{1max} & \varphi \geq \varphi_1(s) \\ f(s,\varphi_b,\varphi_1,\varphi_2) & \varphi_2(s) \leq \varphi_b \leq \varphi_1(s) \\ f(s,\varphi_b,\varphi_2,\varphi_3) & \varphi_3(s) \leq \varphi_b \leq \varphi_2(s) \\ f(s,\varphi_b,\varphi_3,\varphi_4) & \varphi_4(s) \leq \varphi_b \leq \varphi_3(s) \\ f(s,\varphi_b,\varphi_4,\varphi_5) & \varphi_5(s) \leq \varphi_b \leq \varphi_4(s) \\ f(s,\varphi_b,\varphi_5,\varphi_6) & \varphi_6(s) \leq \varphi_b \leq \varphi_5(s) \\ \varphi_{6max} & \varphi < \varphi_6(s) \end{cases} \tag{8}$$

Where, corresponding to the braking force system values of dry asphalt, dry cement, wet asphalt, wet cobblestone, snow and ice pavement; F is the identification algorithm of road surface peak adhesion coefficient adopted in this paper.

Determine the quantitative relationship between different slip rates, braking force coefficients and the peak adhesion coefficient of the road surface. After sorting out the data, fit the data points to draw the surface map of the peak coefficient, as shown in Fig. 5.

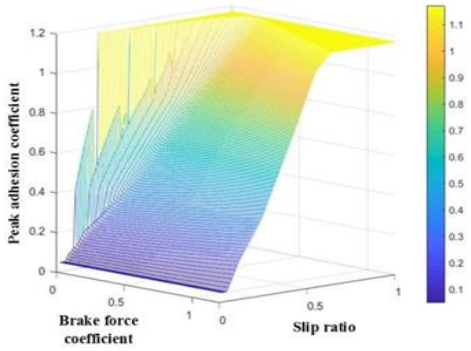

Fig. 5. Surface with peak adhesion coefficient.

In order to test the pavement identification effect, the adhesion coefficient of the simulated road was set as 0.3 in the CarSim, the initial speed was set as 50km/h, the braking pressure increased from 0MPa to 10MPa in the period of 1-5s, and other parameters remained the default setting. The simulation test results were shown in Figure 6.

As can be seen from Figure 6, during 1s to 2s of the braking process, there was a large error in the identification of the peak adhesion coefficient of the road surface. Then the ABS started to work and the identification data of the peak adhesion coefficient of the road surface stabilized to 0.3. It can be seen that when the slip rate fluctuates within the range of 0.1 to 0.4, the identification result of the peak adhesion coefficient of road surface is relatively stable, and the identification error is less than 0.02. With the decrease of the vehicle speed, the slip rate fluctuates to a low slip rate range, and the identification results appear large errors again. The above results show that this method can achieve a more accurate estimation of the peak adhesion coefficient when the slip rate is within the range of 0.1 to 0.4, which is in line with the design expectation. Because the identification error within the range of low slip rate is too large, the slip rate threshold value is set, and the road surface identification is not carried out below the threshold value.

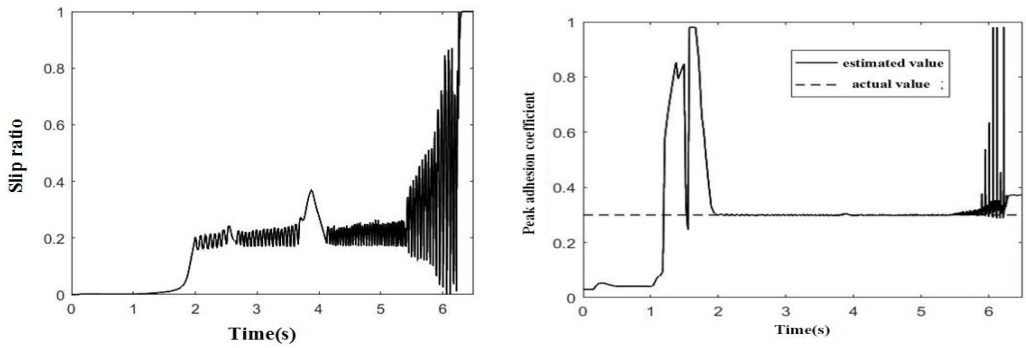

(a) Wheel slip ratio (b) Peak adhesion coefficient of road surface

Fig. 6. Surface with peak adhesion coefficient.

III. ACTIVE COLLISION AVOIDANCE SAFETY MODEL

A. *Minimum Braking Distance*

In the process of longitudinal braking for collision avoidance, if the slip rate rises suddenly after braking, it indicates that there is a risk reduction in the braking efficiency of the self-propelled vehicle. At this time, the ABS of the self-propelled vehicle is opened accordingly, forcing the slip rate of the wheel to be near the slip rate corresponding to the peak adhesion coefficient.By using this feature and combining with the road adhesion coefficient estimation method described above, the peak adhesion coefficient of the current road can be quickly estimated. Then, according to the information of the current self-vehicle speed and the speed of the vehicle in front, the shortest braking distance of longitudinal braking that can be achieved by the maximum braking capacity of the current road can be calculated. If the current workshop distance is less than the shortest braking distance, it indicates that longitudinal braking can no longer achieve collision avoidance, then steering lane change can be adopted to avoid collision, to improve the vehicle collision avoidance ability.

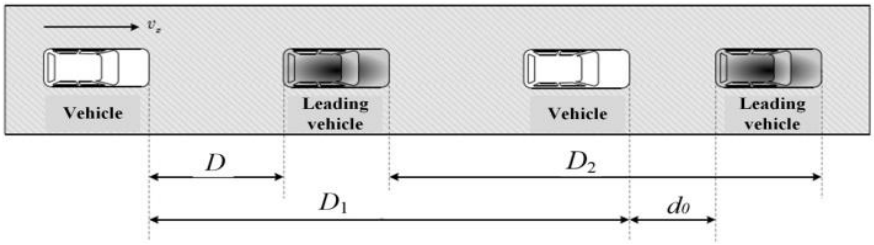

Fig. 7. Longitudinal braking process workshop distance.

In the process of longitudinal braking for collision avoidance, the distance changes between the vehicle and the vehicle in front are shown in Fig. 7. In Fig. 7, D is the initial workshop distance between the vehicle in front and the vehicle in front before braking for collision avoidance; D_1 is the distance traveled by the autonomous vehicle in the whole collision avoidance process; D_2 is the distance traveled by the leading vehicle in the process of collision avoidance; D_0 s the safe distance between the vehicle in front and the vehicle in front after the end of collision avoidance.

Assume that the maximum braking deceleration speed a_{1max} that can be achieved by the autonomous vehicle in the braking process is [3].

$$a_{1\max} = \mu g \tag{9}$$

Where, μ is the road adhesion coefficient.

The estimated value of peak adhesion coefficient φ max is taken as the adhesion coefficient of the current road surface and substituted into Equation 9 to obtain the maximum braking deceleration speed of the current vehicle, and the calculation of the latest braking distance of the vehicle can be described as.

$$D_{1pb} = D_1 - D_2 + d_0 \tag{10}$$

Where, D_0 is the safety distance; D_1 is shown in Equation 11; D_2 is shown in Equation 12.

$$D_1 = \frac{v_1^2 - v_2^2}{2a_{1\max}} \tag{11}$$

$$D_2 = \begin{cases} v_2 \dfrac{v_1 - v_2}{a_1} & a_2 = 0, v_2 \geq 0 \\ \dfrac{v_2^2}{2a_2} & a_2 < 0, v_2 > 0 \\ v_2 \dfrac{D}{v_1 - v_2} + \dfrac{1}{2} a_2 \left(\dfrac{D}{v_1 - v_2} \right)^2 & a_2 < 0, v_1 > v_2 \end{cases} \tag{12}$$

Where, v_1 is the vehicle speed; v_2 is the speed of the vehicle in front; a_1 is the acceleration of self-propelled vehicle; a_2 is the acceleration of the car in front.

B. *Minimum Steering Distance*

In this paper, the curve of quintic polynomial function is selected as the collision avoidance trajectory. The trajectory has the characteristics of second-order continuity, continuous curvature, smooth, no mutation, and easy to impose constraints. It is suitable for the lane change control of steering and collision avoidance when the front and rear vehicles are in the same lane driving in a straight line.

The collision avoidance trajectory equation is shown in Equation 13.

$$\begin{cases} Y = W \left[10 \times \left(\dfrac{x}{d} \right)^3 - 15 \times \left(\dfrac{x}{d} \right)^4 + 6 \times \left(\dfrac{x}{d} \right)^5 \right] & (0 < x \leq d) \\ Y = W & (x > d) \end{cases} \tag{13}$$

Where, W is the lateral displacement at the end of the track. In this paper, the width of the standard lane is 3.75m. Y is the lateral displacement of vehicle center of mass; X is the longitudinal displacement of vehicle center of mass; D is the length of collision avoidance trajectory.

In the process of vehicle tracking collision avoidance trajectory, the maximum lateral acceleration needs to be constrained, and the maximum lateral acceleration needs to be solved by first obtaining the curvature k from the curvature equation of collision avoidance trajectory, as shown in Equation 14.

$$k = \frac{W \left(120 \dfrac{x^3}{d^5} - 180 \dfrac{x^2}{d^4} + 60 \dfrac{x}{d^3} \right)}{\left\{ 1 + W^2 \left(30 \dfrac{x^4}{d^5} - 60 \dfrac{x^3}{d^4} + 30 \dfrac{x^2}{d^3} \right) \right\}^{3/2}} \tag{14}$$

The relationship between the curvature of vehicle driving curve and lateral acceleration of vehicle is shown in Equation 15.

$$a_y = k v_1^2 \tag{15}$$

By analyzing the test data, Nathaniel limited the maximum lateral acceleration of the vehicle in the process of steering and lane changing to the circumference shown in Equation 16 [4]. In order to improve the application range of steering collision avoidance as much as possible, the maximum allowable lateral acceleration of steering collision avoidance is set as $0.85\mu g$.

$$0.67\mu g \leq a_y \leq 0.85\mu g \tag{16}$$

Due to the simulation and experimental process, the real time operation requires a certain amount of time the shortest collision avoidance curve, and the urgent need in the process of collision avoidance to minimize the time the losses resulting from the operation, this paper will advance different maximum curvature corresponding

collision avoidance curve length was calculated and the summary data into the table, the working process of the system in the vehicle has been set, the lateral acceleration, then, the maximum curvature of the collision avoidance trajectory is determined according to Equation 15. Then, the trajectory length is obtained by searching the collision avoidance trajectory table, as shown in Fig. 8, and the shortest collision avoidance trajectory under the constraint of maximum lateral acceleration is determined m^{-1}.

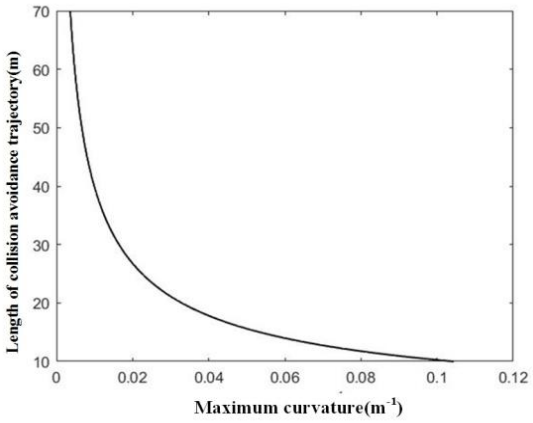

Fig. 8. Maximum curvature and collision avoidance trajectories.

After determining the shortest collision avoidance trajectory, it is necessary to determine the latest steering distance. As the driving conditions of the leading vehicle are complex and changeable, it is difficult to predict. In order to ensure safety, the calculation of the latest steering distance always assumes that the leading vehicle remains stationary. In order to ensure that there is no collision with the front vehicle in the process of steering lane change to avoid collision, the body position in the process of steering collision avoidance needs to be analyzed. As shown in Fig. 9 and Fig. 10, because the front part of the vehicle is farther from the steering center, the outside front corner of the vehicle is most likely to collide with the front vehicle in the process of steering lane change to avoid collision. Therefore, in the process of lane change for collision avoidance, the condition that the vehicle does not collide with the vehicle in front is that when the lateral displacement of the lateral front Angle of the vehicle is equal to the width of the vehicle in front or the obstacle, there is still a certain distance between the vehicle and the vehicle in front [5].

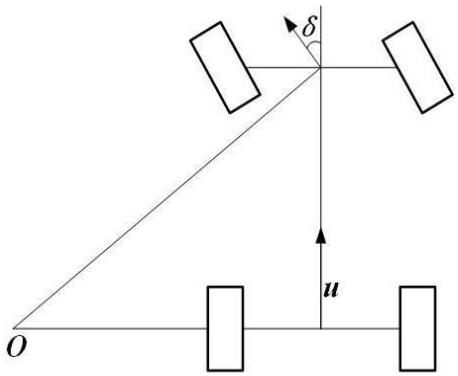

Fig. 9. The steering motion of a car.

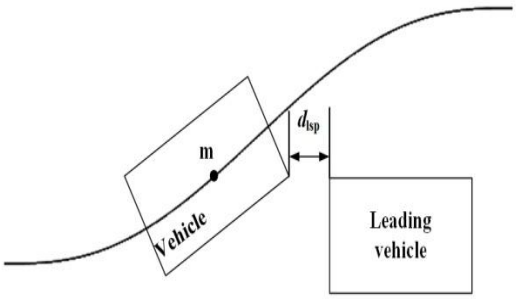

Fig. 10. No collision condition for the vehicle.

According to the above conditions, in order to determine the shortest collision avoidance trajectory in the tracking process and the position of the center of mass of the self-vehicle when the lateral displacement of the outside front corner of the self-vehicle is the same as the width of the front vehicle and there is no collision, the

coordinates of the outside front corner need to be expressed by the center of mass coordinates [6]. In this paper, the vehicle is simplified into a rectangle. Then, the geometric relationship between the outside front Angle of the vehicle and the position of the center of mass in the geodetic coordinate system is shown in Figure 11.

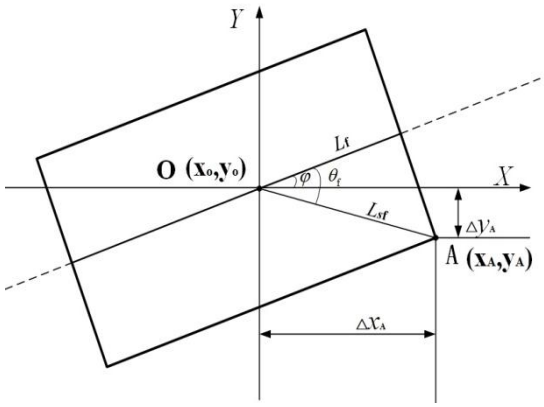

Fig. 11. The geometrical relationship between the center of mass and the front Angle of the auto vehicle.

L_f in Fig. 11 is the distance from the center of mass of the vehicle to the head; L_{sf} is the distance from the vehicle's center of mass to the outside front corner; θ_f is the included Angle between L_f and L_{sf}. The above parameters can be obtained directly or calculated by vehicle parameters in CarSim. The center of mass O is (xo, yo).

Since the vehicle is within the limit range of lateral acceleration, the deviation generated in the tracking process of collision avoidance trajectory is generally small. At the same time, for the convenience of solving the coordinates of point A(XA, YA), the heading Angle φ in the course of steering collision avoidance is expressed by Equation 17.

$$\varphi = \arctan(30\times\frac{W\cdot x^2}{d^3} - 60\times\frac{W\cdot x^3}{d^4} + 30\times\frac{W\cdot x^4}{d^5}) \tag{17}$$

According to the geometric relationship, the coordinates of point A can be expressed by Equation 18.

$$\begin{cases} x_A = x_o + L_{sf}\times\cos(\theta_f - \varphi) \\ y_A = y_o - L_{sf}\times\sin(\theta_f - \varphi) \end{cases} \tag{18}$$

According to Equation 18, the position of the center of mass can be obtained when the lateral displacement of the outside front corner of the vehicle is the width of the vehicle in front. The distance between the center of mass position of the vehicle and the center of mass position of the vehicle at the beginning of steering collision avoidance along the X-axis direction is the shortest steering limit distance D_{ulsp}. In order to ensure safety, a certain safety distance D_{lsp} should be reserved. The shortest turning distance D_{LSP} can be expressed by Equation 19.

$$D_{lsp} = D_{ulsp} + d_{lsp} \tag{19}$$

In this paper, the least square method was used in advance to pre-calculate the shortest ultimate steering distance corresponding to multiple collision avoidance trajectory curves, so as to refer to the table during operation. The obtained shortest ultimate steering distance corresponding to different collision avoidance trajectory is shown in Fig. 12.

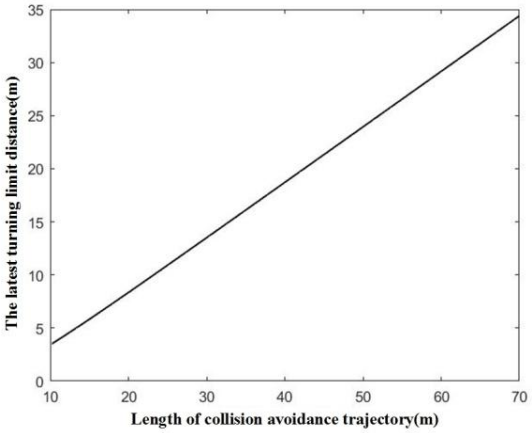

Fig. 12. Length of collision avoidance trajectory and minimum steering limit distance.

C. *Collision Avoidance Trajectory Planning*

After the latest braking distance and the latest steering distance are determined, the entire collision avoidance range can be divided into three areas, as shown in Figure 13.

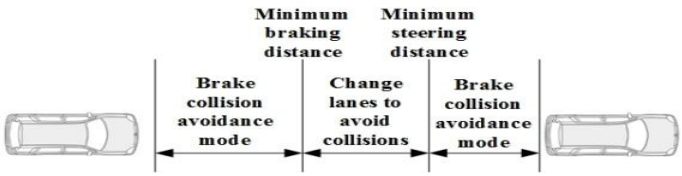

Fig. 13. Collision avoidance method division.

When workshop distance in collision avoidance area to flow, trajectory planning for collision avoidance, aims at realizing the premise of collision avoidance, as far as possible a more gentle lane changing trajectory, on the one hand, to promote the process of collision avoidance comfort, on the other hand can reduce the collision avoidance lateral acceleration of the process, try to avoid in the process of steering collision avoidance produce sideslip vehicles such as unstable phenomenon [7].

Use system trigger to collision avoidance of workshop and set aside a safe distance, shown in figure 12, according to the length and the shortest collision avoidance trajectory distance limit corresponding relational tables, through to limit shortest distance to find corresponding collision avoidance trajectory method can get a certain safe distance and the length of the lateral acceleration small collision avoidance path as far as possible.

IV. A Simulation Verification of Active Collision Avoidance System

In order to test the effect of active collision avoidance decision, this paper adopts the TTC model, the longitudinal collision avoidance control with two-stage braking strength and the trajectory tracking control with model prediction to realize the steering and lane change for collision avoidance. Due to the space limitation, the above two controls will not be discussed.

In order to verify the performance of longitudinal collision avoidance control on road surfaces with different adhesion conditions, the road adhesion coefficient was set as 0.8 and 0.4, respectively. The autonomous vehicle drove along the straight road at a initial velocity of 70km/h, and an obstacle vehicle was set to stop stationary in the lane 40m ahead of the autonomous vehicle. The simulation results were shown in Figure 14 and 15.

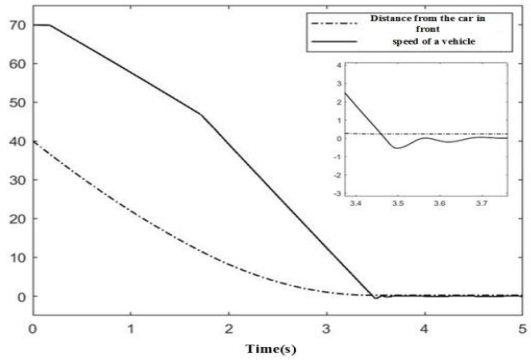

Fig. 14. Simulation results of longitudinal collision avoidance on high adhesion road surface.

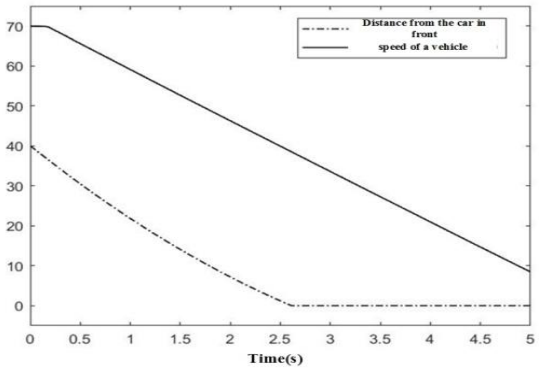

Fig. 15. Simulation results of longitudinal collision avoidance on low adhesion road surface.

As can be seen from Figure 14 and 15, on the high adhesion road surface, the self-employed vehicle successfully reduces the speed of the self-employed vehicle to zero through two-stage braking and maintains a safety distance of about 0.3m between the self-employed vehicle and the stationary front vehicle, thus successfully avoiding a collision.On the low adhesion road surface, the longitudinal braking control effect of the self-employed vehicle was obviously insufficient, and the self-employed vehicle collided with the front vehicle at about 2.6s time.

In order to solve the problem of decreasing effect of longitudinal braking control on low-adhesion road surface, the active collision avoidance decision estimated by road peak adhesion coefficient was adopted to carry out simulation tests on the above-mentioned low-adhesion road surface. The simulation results are shown in Fig. 16.

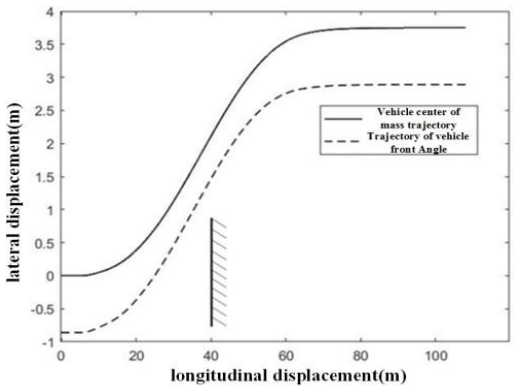

(a) The center of mass, the track of the outside front Angle and the position of the obstacle.

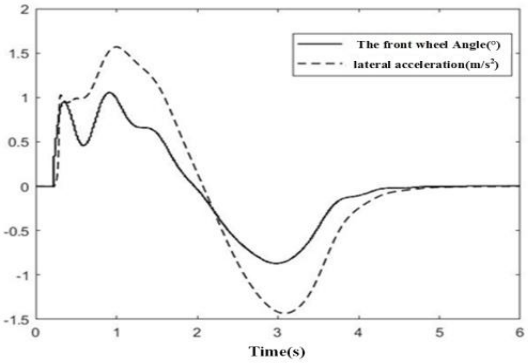

(b) Front wheel Angle and lateral acceleration

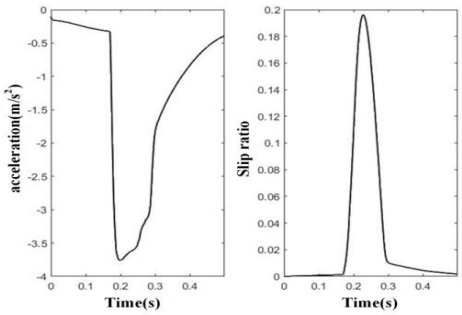

(c) Longitudinal acceleration and wheel slip rate

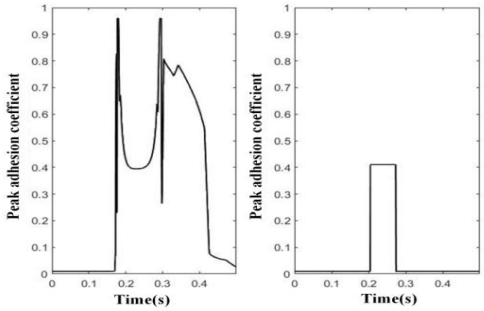

(d) The pavement identification result and the result after treatment

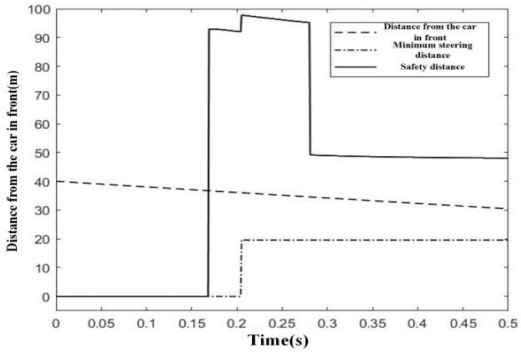

(e) The output value of the safety distance model is compared with the distance of the workshop.

Fig. 16. Results of active collision avoidance test on low adhesion road surface.

As can be seen from Fig. 16(a), after driving in a straight line for a certain distance, the autonomous vehicle avoids the obstacles in front by turning. The trajectory of the outside front corner of the autonomous vehicle

indicates that the autonomous vehicle does not collide with the obstacles during the whole collision avoidance process, and the autonomous vehicle safely switches to the left lane and continues to drive forward. As can be seen from Fig. 16(b), the self-driving vehicle starts to turn at about 0.3s. During the lane change process, the maximum front wheel rotation Angle is about 1° and the maximum lateral acceleration is about 1.5m/s2, indicating that the vehicle runs smoothly in the process of collision avoidance and ensures a certain comfort. As can be seen from Fig. 16(c), the autonomous vehicle has carried out longitudinal braking before steering, resulting in a certain deceleration. Due to the low road adhesion coefficient, the wheel slip ratio increases accordingly.As can be seen from Fig. 16(d), due to the increase of slip rate, the system began to identify the peak adhesion coefficient of road surface and processed the identification results. The processed identification results more accurately estimated the current pavement adhesion conditions. From figure 16 (e), the safety distance model receives the road recognition results, at about 0.2 s safe distance estimation results rise to about 100 meters, show that the current pavement can provide braking deceleration is smaller than the current expectations of braking deceleration, braking distance and the shortest distance is greater than the current workshop, the workshop distance is greater than the shortest distance, Successfully take the steering decision to avoid collision.

V. CONCLUSION

In this paper, an active collision avoidance decision method based on the estimation of peak adhesion coefficient of road surface is proposed. Firstly, the method of estimating the adhesion coefficient of the peak road surface is introduced, and then the shortest braking distance is calculated by using the result of road surface estimation. Then, the shortest steering distance is obtained and the trajectory planning is realized by geometric analysis and numerical calculation under the condition that the outside front Angle of the vehicle does not collide with the vehicle in the course of steering collision avoidance trajectory tracking. Finally, the real-time simulation results show that when the main vehicle can not achieve the expected effect of collision avoidance, it can recognize the road conditions autonomously and make reasonable steering decisions and actions in time to avoid collision, and successfully achieve collision avoidance. At the same time, due to the planning of collision avoidance trajectory, the whole process of collision avoidance is stable and comfortable.

REFERENCES

[1] Zhu Bing,Piao Qi,Zhao jian. Vehicle longitudinal collision warning strategy based on road adhesion coefficient estimation [J]
[2] Fahrwerktechnik B M. Radschlupf-Regelsysteme. Weirzburg: Vogel Verlag,1993
[3] Li Lin, Zhu Xichan, Chen Hailin. Driver braking and steering avoidance limits [J] Journal of Tongji University (Natural Science Edition), 2016. 44(11): 1743-1748.
[4] Sledge NH. An investigation of vehicle critical speed and its influence on lane-change trajectories [D]. The University of Texas at Austin, 1997.
[5] Wang Kai. Research on lane change assistant system based on model predictive control [D]. Hefei: Hefei University of Technology, 2018.
[6] Feng Haipeng. Research on modeling and control strategy of automobile automatic emergency braking system [D]. Jiangsu: Jiangsu University, 2019.
[7] Lian Yufeng. Research on state estimation and control strategy of active collision avoidance system for electric vehicles [D]. Changchun: Jilin University, 2015.

AUTHOR'S PROFILE

First Author
Shi Peilin, Doctor of Engineering, Male, Associate professor. School of Transportation and Vehicle Engineering, Shandong University of Technology, Shandong, Zibo, Zhangdian, 255049 (First author), China. You can contact with Peilin Shi, Thank you! email id: ericshi65@163.com.

Second Author
Longhui Zhou, Master in reading, Male, School of Transportation and Vehicle Engineering, Shandong University of Technology, Shandong, Zibo, Zhangdian, 255049, China. You can contact with the Zhou Longhui, Thank you! email id: 759767868@qq.com

Third Author
Hou Jianwei, Master in reading, Male, School of Transportation and Vehicle Engineering, Shandong University of Technology, Shandong, Zibo, Zhangdian, 255049, China.

Fourth Author
Minglei Liang, Master in reading, Male, School of Transportation and Vehicle Engineering, Shandong University of Technology, Shandong, Zibo, Zhangdian, 255049, China.

Fifth Author
Liaodong Zheng, Master in reading, Male, School of Transportation and Vehicle Engineering, Shandong University of Technology, Shandong, Zibo, Zhangdian, 255049, China.

Sixth Author
Yushuai Zhao, Master in reading, Male, School of Transportation and Vehicle Engineering, Shandong University of Technology, Shandong, Zibo, Zhangdian, 255049, China.